Structural Chemistry (2022) 33:1189–1197
https://doi.org/10.1007/s11224-022-01927-x

ORIGINAL RESEARCH

Synthesis, computational analyses, antibacterial and antibiofilm properties of nicotinamide derivatives

Ayşe Hümeyra Taşkın Kafa[1] · Gamze Tüzün[2] · Elif Güney[2] · Rukiye Aslan[1] · Koray Sayın[2] · Burak Tüzün[3] · Hilmi Ataseven[4]

Received: 7 March 2022 / Accepted: 24 March 2022 / Published online: 4 April 2022

Abstract

Newly designed nicotinamide derivatives were synthesized and characterized using spectral techniques (IR, ^{1}H-NMR, ^{13}C-NMR, and MS). Moreover, these compounds are investigated computationally. B3LYP/6–31 + G(d,p) level is selected as the calculation level in this study. Experimental and calculated IR spectrum were compared to each other. Electronic properties of synthesized compounds are examined using HOMO/LUMO contour plot and MEP maps. Antibacterial activity and antibiofilm properties are investigated experimentally. Additionally, antibacterial properties of studied compounds are investigated by molecular docking analyses. As a result, ND4 was found as the best inhibitor candidate against *Enterococcus faecalis*.

Keywords Nicotinamide · Synthesis · DFT · Docking · Antibacterial studies

Introduction

Nicotinamide which is an amide derivative of nicotinic acid has over the past 50 years been investigated for a variety of biological applications [1–4]. Nicotinamide is also known as vitamin B_3 and a component of nicotinamide adenine dinucleotide (NAD). Nicotinamide is currently in the trial as preventing Type I diabetes and has antibacterial, antimicrobial, antifungal, anti-HIV, and anti-pesticide properties [4–10]. In addition to these features, nicotinamide has anti-dandruff, anti-itching, hair growth-promoting, gray hair preventing, increasing hair elasticity, and treating acne, fine lines as well as age spots properties [4]. As can be seen, it is understood that nicotinamide and its derivatives have a wide biological application range.

In this study, four nicotinamide derivatives which are 2-chloro-*N*-(2-chlorophenyl)nicotinamide (**ND1**), 2-chloro-*N*-(3-chlorophenyl)nicotinamide (**ND2**), 2-chloro-*N*-(4-chlorophenyl)nicotinamide (**ND3**), and *N*-(2-bromophenyl)-2-chloronicotinamide (**ND4**) are investigated computationally and experimentally. Initially, these compounds are synthesized and characterized using spectral techniques (IR, ^{1}H-NMR, ^{13}C-NMR, and MS). Then, these compounds are optimized at B3LYP/6–31 + G(d,p) level in water with the C-PCM solvent method. Electronic properties of these compounds are examined using contour plots of frontier molecular orbital and molecular electrostatic potential (MEP) map of them. In vitro antibacterial and antibiofilm (or biofilm inhibition) activity of the synthesized compounds are tested against Gram-positive bacteria *S. aureus* (ATCC 29,213), Methicillin-resistant *Staphylococcus aureus* (ATCC 43,300), *Enterococcus faecalis* (ATCC 29,212) and Gram-negative bacteria *E. coli* (ATCC 25,922), *P. aeruginosa* (ATCC 27,853), *Klebsiella pneumoniae* (ATCC 700,603). The compounds are also screened for antifungal activity against *C. albicans* (ATCC 10,231).

✉ Koray Sayın
krysayin@gmail.com

[1] Department of Medical Microbiology, Faculty of Medicine, Cumhuriyet University, Sivas, Turkey

[2] Department of Chemistry, Faculty of Science, Sivas Cumhuriyet University, Sivas, Turkey

[3] Department of Plant and Animal Production, Technical Sciences of Sivas Vocational School, Sivas Cumhuriyet University, Sivas, Turkey

[4] Department of Gastroenterology, Faculty of Medicine, Sivas Cumhuriyet University, Sivas, Turkey

Materials and methods

Reagents

2-chloronicotinoyl chloride, 2-chloroaniline, 3-chloroaniline, 4-chloroaniline, 2-bromoaniline, triethylamine and solvents which are dichloromethane (DCM), 1,2-dichloroethane (1,2-DCE), chloroform, petroleum ether, diethyl ether, DMSO was purchased from Merck kGaA.

Instrumentation

IR spectra (4000–400 cm^{-1}) were obtained using IR spectra (ATR) and recorded on a Bruker Tensor II FT-IR spectrometer. Melting points were measured on an Electrothermal IA9100 apparatus. ^{1}H-NMR and ^{13}C-NMR spectra were recorded on a JEOL (400 MHz) JNM-ECZ400S/L1 NMR instrument in DMSO-d_6 at room temperature; δ in ppm relative to tetramethylsilane (TMS), with J in hertz (Hz). Agilent Technology Inc. of 1260 Infinity HPLC System was coupled with 6530 Q-TOF LC/MS detector and ZORBAX SB-C18 (2.1 × 50 mm, 1.8 µm) column. ^{1}H-NMR, ^{13}C-NMR, and Q-TOF LC/MS analyses of the compounds were carried out at the Advanced Technology Application and Research Center (CUTAM) of Sivas Cumhuriyet University.

Synthesis of nicotinamide derivatives

Four nicotinamide derivatives were synthesized in one step. Schematic illustration of the synthesis was represented in Fig. 1. Additionally R groups in synthesized compounds are given in Table 1. Mentioned aniline derivatives are added to the solution of 2-chloronicotinoyl chloride in DCM:1,2-DCE (1:1) with trimethylamine. The mixture were refluxed for three hours and extracted with CH_2Cl_2. The organic part was dried Na_2SO_4 and evaporated. The residue was crystallized in ethanol/$CHCl_3$ (8:2).

The compounds, which are ND1–ND4 given above, were synthesized and their spectral characterizations (IR, ^{1}H-NMR, ^{13}C-NMR, and LC-QTOF-MS) were performed. The related spectrum were given in Supp. Material. The spectral data obtained were given as follow for each synthesized compounds:

Table 1 R group in synthesized compound

Assignment	R_1	R_2	R_3
ND1	Cl	H	H
ND2	H	Cl	H
ND3	H	H	Cl
ND4	Br	H	H

2-chloro-*N*-(2-chlorophenyl)nicotinamide (**ND1**): yield: 74%. Off-white crystal. IR (cm^{-1}): 3260, 3214, 3033, 1654, 1580, 1526, 1475, 1439, 1402, 1309, 1147, 1065, 987, 947, 910, 847, 815, 746, 687, 649, 600, 534, 488, 445. ^{1}H NMR (400 MHz, CHLOROFORM-*D*) δ 8.78, 8.56 – 8.44 (m, 2H), 8.23 (dd, *J* = 7.7, 1.9 Hz, 1H), 7.42 – 7.38 (m, 2H), 7.35 – 7.29 (m, 1H), 7.13 – 7.07 (m, 1H). ^{13}C NMR (101 MHz, CHLOROFORM-D) δ 162.59, 151.66, 147.13, 140.44, 134.26, 131.04, 129.38, 127.93, 125.66, 123.60, 123.07, 122.09. HPLC-TOF/MS: 264.9934 ($[M-H]^-$, $C_{12}H_8Cl_2N_2O^-$; calc. 264.9941).

2-chloro-*N*-(3-chlorophenyl)nicotinamide (**ND2**): yield: 87%. Off-white crystal. IR (cm^{-1}): 3381, 3278, 3016, 2864, 1663, 1615, 1584, 1548, 1477, 1425, 1401, 1335, 1281, 1154, 1069, 916, 865, 806, 785, 752, 685, 661, 616, 557, 440. ^{1}H NMR (400 MHz, DMSO-D_6) δ 10.42, 8.10, 7.65 (d, *J* = 7.6 Hz, 1H), 7.46, 7.15 – 7.09 (m, 2H), 6.94 (t, *J* = 8.1 Hz, 1H), 6.74 (d, *J* = 8.3 Hz, 1H). ^{13}C NMR (101 MHz, DMSO-D_6) δ 163.74, 150.61, 146.25, 139.92, 138.14, 133.07, 132.64, 130.51, 123.74, 123.07, 118.91, 117.88. HPLC-TOF/MS: 264.9939 ($[M-H]^-$, $C_{12}H_8Cl_2N_2O^-$; calc. 264.9941).

2-chloro-*N*-(4-chlorophenyl)nicotinamide (**ND3**): yield: 69%. Off-white crystal. IR (cm^{-1}): 3285, 3106, 3064, 2081, 1986, 1942, 1893, 1660, 1578, 1513, 1396, 1312, 1243, 1135, 1088, 1064, 1014, 904, 820, 744, 689, 508, 419. ^{1}H NMR (400 MHz, DMSO-D_6) δ 10.74, 8.49 (dd, *J* = 4.8, 1.9 Hz, 1H), 8.04 (dd, *J* = 7.6, 2.0 Hz, 1H), 7.69 (d, *J* = 2.1 Hz, 1H), 7.67 (d, *J* = 2.1 Hz, 1H), 7.52 (dd, *J* = 7.5, 4.8 Hz, 1H), 7.39 (d, *J* = 2.1 Hz, 1H), 7.37 (d, *J* = 2.1 Hz, 1H). ^{13}C NMR (101 MHz, DMSO-D_6) δ 164.17, 151.19, 146.95, 138.78, 138.14, 133.45, 129.36, 128.24, 123.74, 121.62. HPLC-TOF/MS: 264.9943 ($[M-H]^-$, $C_{12}H_8Cl_2N_2O^-$; calc. 264.9941).

N-(2-bromophenyl)-2-chloronicotinamide (**ND4**): yield: 72%. Off-white crystal. IR (cm^{-1}): 3269, 3215, 3028, 2084, 1882, 1654, 1578, 1521, 1473, 1436, 1400, 1305, 1145,

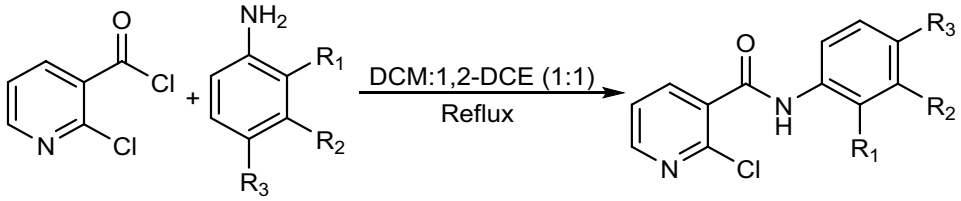

Fig. 1 Synthesis schema

1125, 1061, 1030, 907, 841, 814, 739, 641, 595, 434. ^{1}H NMR (400 MHz, CHLOROFORM-*D*) δ 8.69, 8.51 (dd, *J* = 4.8, 2.1 Hz, 1H), 8.47 (d, *J* = 8.4 Hz, 1H), 8.25 – 8.16 (m, 1H), 7.57 (dd, *J* = 8.0, 1.6 Hz, 1H), 7.44 – 7.32 (m, 2H), 7.04 (td, *J* = 7.7, 1.7 Hz, 1H). ^{13}C NMR (101 MHz, CHLOROFORM-*D*) δ 162.70, 151.65, 147.16, 140.32, 135.40, 132.66, 131.15, 128.57, 126.19, 123.05, 122.45, 114.05. HPLC-TOF/MS: 308.9449 ($[M-H]^-$, $C_{12}H_8ClBrN_2O^-$; calc. 308.9436).

Computational chemistry

The Gaussian software was used in the computational investigations [11, 12]. The synthesized compounds were fully-optimized at the B3LYP method with 6–31 + G(d,p) basis set in water. In this stage, conductor-like polarizable continuum model (C-PCM) was used as solvent model to consider solute–solvent interactions. At the results of calculations, no imaginary frequency was observed. IR and NMR spectrum were calculated at the same level of theory. Additionally, electronic properties of these compounds are examined using contour plots of frontier molecular orbitals and moleculer electrostatic potential (MEP) map. Some utilities such as the ChemDraw software were used as utility in this study [13].

Antimicrobial activity

In vitro antibacterial activity of the synthesized compounds was tested against Gram-positive bacteria; *Staphylococcus aureus* (ATCC 29213), Methicillin-resistant *S. aureus* (ATCC 43300), *Enterococcus faecalis* (ATCC 29212), and Gram-negative bacteria; *Escherichia coli* (ATCC 25922), *Pseudomonas aeruginosa* (ATCC 27853), *Klebsiella pneumoniae* (ATCC 700603). The compounds were also screened for antifungal activity against *Candida albicans* (ATCC 10231). The stock solutions of compounds were prepared in dimethyl sulfoxide (DMSO) at a concentration of 2 mg/ml. The Minimum Inhibitory Concentration (MIC) values of compounds were determined using the micro-broth dilution method in 96-well microtiter plates [14]. Test compounds were serially diluted in Muller Hinton Broth (MHB). The ciprofloxacin antibiotic to bacteria and fluconazole antimycotic to fungus used for positive controls. The microplates were incubated at 37 °C for 24 h. All of the studies were applied in triplicate, and the results were provided as mean values.

Biofilm inhibition assay

The synthesized compounds were screened in sterile 96-well polystyrene micro-titer plates using the biofilm inhibition assay against a panel of pathogenic strains which were cultured overnight in tryptone soy broth (TSB) (supplemented with 2% glucose) [15].

The test compounds of predetermined MIC concentrations ranging from 500 to 1000 µg/ml were mixed with the bacterial suspensions having an initial inoculums concentration of 5×10^5 CFU/mL. One hundred microliters of compound solution and 100 µL of 0.5 McFarland (10^8 CFU/ml) turbid bacteria suspension were added to 96-well U-bottom microplates. Only 200 µL of bacterial suspension was added to the wells for positive control. Then, the microplates were incubated at 37 °C for 48 h. At the end of the time, all wells were washed 3 times with phosphate-buffered saline (PBS), and non-adherent cells were removed. Then, the biofilm structure in the wells was fixed with 95% methanol for 15 min. The microplates were dried at room temperature. Then, 200 µL of 0.1% crystal violet was added to the wells and incubated for 30 min at room temperature. Then, 200 µL of 0.1% crystal violet was added to the wells and incubated for 30 min at room temperature. At the end of this time, the

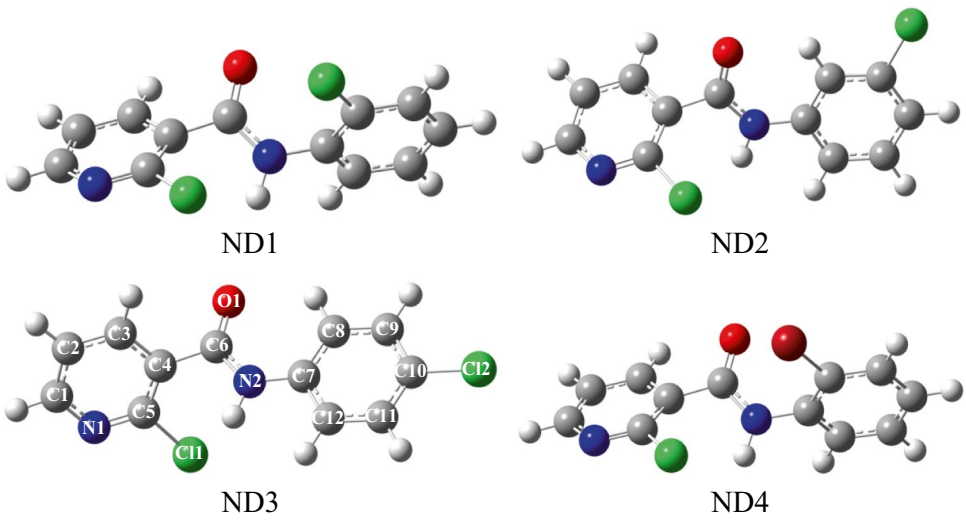

Fig. 2 The optimized structure of studied nicotinamide derivatives

Table 2 The geometric parameters of synthesized compounds at B3LYP/6–31 + G(d,p) level

Assignments	ND1	ND2	ND3	ND4
Bond lengths (Å)				
C1-N1	1.344	1.335	1.342	1.342
C1-C2	1.391	1.394	1.394	1.392
C5-Cl1	1.760	1.772	1.772	1.770
C4-C6	1.504	1.496	1.510	1.501
C6-O1	1.230	1.233	1.230	1.233
C6-N2	1.361	1.362	1.361	1.363
C7-N2	1.421	1.412	1.413	1.424
C7-C8	1.399	1.402	1.399	1.400
Bond angle (deg.)				
C1-N1-C5	118.3	118.0	118.0	118.3
C1-C2-C3	118.0	118.1	118.2	118.0
C3-C4-C6	116.3	117.8	117.9	116.4
C4-C6-O1	119.9	120.1	120.1	119.7
C4-C6-N2	117.0	115.3	115.2	117.2
C6-N2-C7	123.8	129.3	129.2	123.8
Dihedral angle (deg.)				
C3-C4-C6-O1	41.0	52.7	-53.6	36.4
C3-C4-C6-N2	−136.1	−124.8	123.8	−140.9
Cl1-C5-C4-C6	0.7	−0.2	0.4	0.1
C7-N2-C6-O1	−1.9	3.9	−3.8	1.5
C6-N2-C7-C12	−110.7	−179.9	−0.8	67.4

wells were washed 3–4 times with distilled water to remove excess dye, and the microplates were air-dried. Thirty-three percent acetic acid solution was added to dissolve the dye in the wells, and biofilm inhibition was measured 20 min later at 570 nm with a UV–Vis spectrophotometer (Bio-Tek, Winooski, USA). The percent of biofilm inhibition was calculated according to the formula below [16]. All experiments were carried out in triplicates and the values are indicated as mean ± S.D.

$$\% \text{ Inhibition} = 100 - \left(\frac{\text{OD570 sample}}{\text{OD570 control}} \times 100 \right)$$

Molecular docking

Molecular docking analyses were performed using the Maestro 12.8 software [17–20]. In this program, some modules which are Protein Preperation, Ligand Preperation, Grid Generation, Site Map, Ligand Docking, and Ligand Interaction were used [17–20]. pH was selected as 7 ± 2. The target protein for docking analyses is selected as 6QXS from protein data bank [21].

Results and discussion

Optimized structures

The synthesized compounds are optimized at B3LYP/6–31 + G(d,p) level in the water and the ground state structure of these compounds is represented in Fig. 2 with atomic labeling. In addition to this result, selected geometric parameters which are bond length (Å), bond angle (deg.), and dihedral angle (deg.) are given in Table 2.

According to Table 2, geometric parameters are similar to each other. However, the structures of studied compounds are not planar. Nearly, benzene rings in studied compounds stand perpendicular to each other.

Experimental and computational IR spectra

IR spectrum is essential technique to determine the functional group and necessary for the characterization of chemicals. Vibrational frequencies of studied compounds are obtained both experimental and computational. Experimental results are given in above sections. In this part, computational and experimental results are compared with each other and assignments are done. The IR results are given in Table 3 for **ND1**–**ND2** compounds. Addiitionally, calculated IR spectrum are represented in Supplemental Material. Calculated frequencies scaled by 0.964 to obtain anharmonic frequency.

Table 3 Vibrational frequencies (cm^{-1}) of some functional groups in studied compounds

Assignments	ND1		ND2		ND3		ND4	
	Exp	Calc	Exp	Calc	Exp	Calc	Exp	Calc
ν_{NH}	3214	3450	3381	3460	3285	3445	3269	3464
ν_{CH}	3033	3090	3016	3091	3064	3090	3028	3094
$\nu_{C=O}$	1654	1640	1663	1639	1660	1635	1654	1630
ν_{C-N}	1580	1482	1584	1510	1578	1508	1578	1504
$\nu_{C=C}$	1147	1266	1154	1375	1396	1375	1400	1374
ν_{C-Cl}	746	1032	785	1030	744	1026	739	1029

NMR spectra

Two deutoreted NMR solvents are used in this study which are dimethyl sulfoxide-d6 (in **ND 2** and **ND3**) and chloroform-d (in **ND1** and **ND4**). When the examined ^{1}H-NMR spectra of the studied compounds (**ND1–ND4**), it is seen that the compounds are stable and at ground state. In the ^{1}H-NMR spectra of the synthesized compounds, the proton of amide group in ND1, ND2, ND3, and ND4 give a singlet at 8.78, 10.42, 10.74, and 8.69 ppm, respectively. In the ^{13}C-NMR spectra, the carbonyl group **ND1**–**ND4** is resonated at 162.59, 163.74, 164.17, 162.70 ppm, respectively.

Electronic properties

Determination of electronic properties of compounds is essential for compounds. As computationally, application area of studied compounds can be determined easily using contour plots of frontier molecular orbital and mol molecular electrostatic potential (MEP). In this project, contour plots of frontier molecular orbitals which are HOMO and LUMO are calculated and represented in Fig. 3.

According to Fig. 3, HOMO electrons are delocalized on mainly benzene ring (not pyridine) the structure of the studied compound. At this point, it is observed that π electrons play an essential role. In LUMO plot, electrons are mainly localized on the whole structure of the molecule.

MEP map can be used in determining the electronic properties of the compounds. While the contour plot of frontier molecular orbitals shows special area that can be active, MEP maps show regions on the compound's surface that can interact. MEP maps of the studied compounds are calculated and represented in Fig. 4.

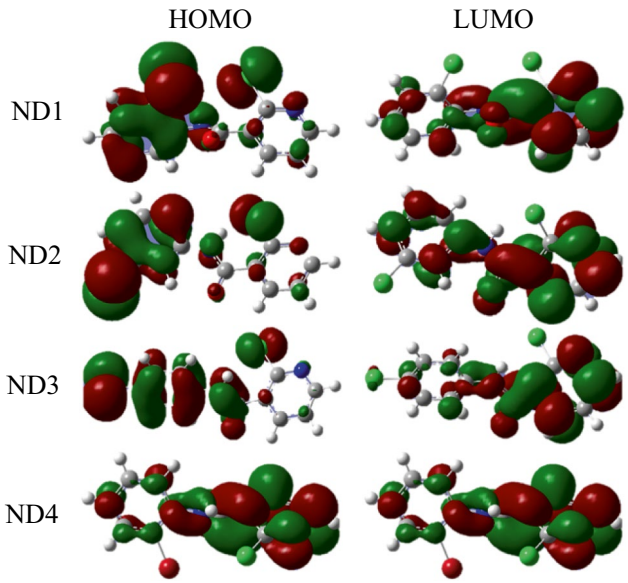

Fig. 3 Contour diagram of frontier molecular orbitals

According to Fig. 4, the surface of compounds is colorful. The observed colors have the meaning of chemically. Red color implies the electron-rich region, while dark blue color implies the electron-poor region. Generally, the environment of oxygen atoms in the carboxyl group is mainly red, and this

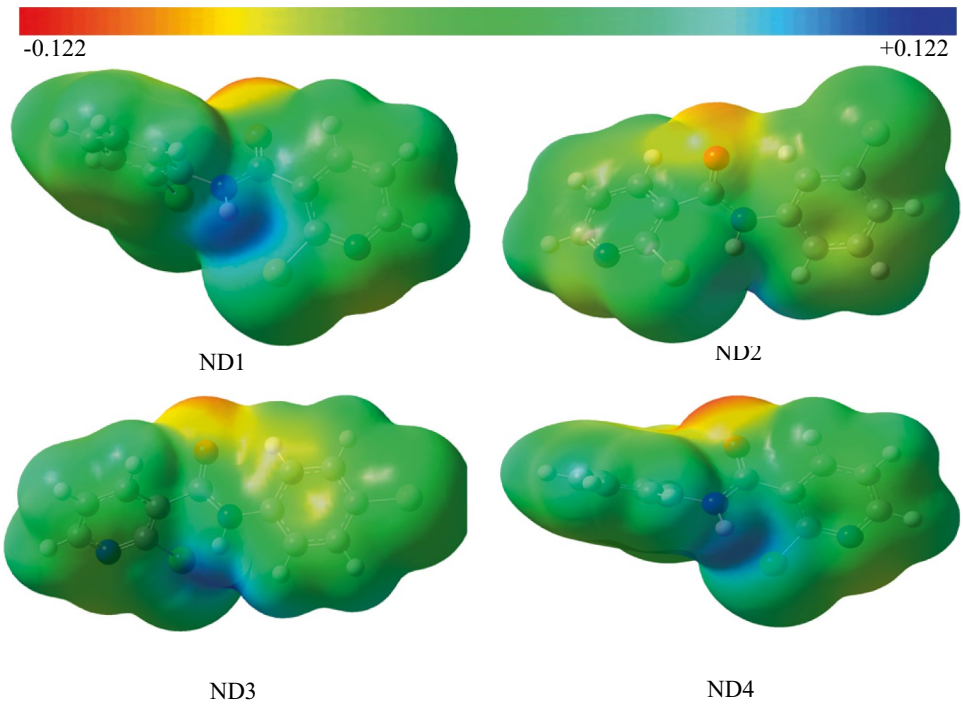

Fig. 4 MEP maps of the studied compounds

Table 4 Antimicrobial screening data of the compounds (MIC in μM)

Compounds	Antibacterial activity						Antifungal activity
	Sa	Mrsa	Ec	Kp	Pa	Ef	Ca
ND1	74.8	74.8	74.8	74.8	74.8	37.4	74.8
ND2	74.8	74.8	74.8	74.8	74.8	37.4	74.8
ND3	74.8	74.8	74.8	74.8	74.8	37.4	74.8
ND4	64.1	64.1	64.1	64.1	64.1	32	64.1
Ciprofloxacin	0.5	1.0	2.0	0.25	0.5	1.0	
Flucanazole							5

Sa Staphylococcus aureus (ATCC 29213), *Mrsa* Methicillin-resistant *S. aureus* (ATCC 43300), *Ef Enterococcus faecalis* (ATCC 29212), *Ec Escherichia coli* (ATCC 25922), *Pa Pseudomonas aeruginosa* (ATCC 27853), *Kp Klebsiella pneumoniae* (ATCC 700603), *Ca Candida albicans* (ATCC10231)

region is appropriate for the electrophilic attack, while the dark blue region is appropriate for the nucleophilic attack.

Antibacterial and antibiofilm activities

Biofilm structure is a growth model that microorganisms form by attaching to a surface and/or each other and embedding in a matrix it produces. Because of this structure, microorganisms gain more resistance to antimicrobials and can develop different strategies to escape from host defense systems [22]. Biofilm-associated infections are serious diseases that are difficult to treat and recurrent. For this reason, it is very important to develop new molecules with antibiofilm properties against biofilm-forming microorganisms. The antimicrobial and antibiofilm activities of newly synthesized compounds were tested in vitro methods against six standard bacterial strains and one yeast, in this study. When Table 4 was examined for the results of the study, it was determined that the compounds ND1, ND2, and ND3 have similar and medium-level (37.4–74.8 μM) antimicrobial activity against microorganisms. The ND4 was found the most effective compound. The most potent effect of this compound was detected against the standard strain of *E. faecalis* (ATCC 29212).

B3 (nicotinamide and nicotinic acid) derivatives, which have antibiotic properties; are of great interest in the treatment of common and life-threatening viral and microbial infections resistant to existing drugs [23]. A remarkable antibacterial effect of a newly synthesized nicotinamide derivative compound against *E. faecalis*, *S. aureus*, *E. coli*, and *P. aeruginosa* bacteria was determined by Adamiec et al. Also, in parallel with our study results, Adamiec et al. detected that the most sensitive bacteria were *E. faecalis*. *P. aeruginosa* was also found to be the most resistant bacteria [24]. Dang et al. determined that pyridoxinium and nicotinium dithiophosphates had strong antibacterial activity (10–20 μM) against *S. aureus*, and antibacterial activity at increasing concentrations ($MIC \geq 320$ μM) against *P. aeruginosa* and *K. pneumoniae* [23].

In this study, it was found that studied compounds have medium and strong antibiofilm activity. When Table 5 is examined, the antibiofilm activity against all tested pathogenic microorganisms was found to be between 3.8–79.8% at ½ MIC concentration values of the compounds. The microorganisms with the strongest inhibition effect against biofilm formation of the compounds were determined as Mrsa (69.6–79.8%) and *C. albicans* (46.2–65.5%).

The microorganism with the lowest activity of the compounds was determined as *K. pneumoniae* (3.2–15.2%).

Kumar et al. stated that pyridine nicotinamide derivatives cause degradation of *Micrococcus luteus* and *S. aureus* biofilm forms, and dispersing of microorganisms, and reported

Table 5 Biofilm inhibition assay of synthesized compounds (MIC/2 in μM)

Compounds	Antibiofilm inhibition %						
	Sa	Mrsa	Ec	Kp	Pa	Ef	Ca
ND1	27.0 ± 0.13	69.6 ± 0.35	41.6 ± 0.19	3.8 ± 0	13.7 ± 0.47	18.3 ± 0.15	60.9 ± 0.08
ND2	31.0 ± 0.17	79.8 ± 0.36	43.0 ± 0.15	4.3 ± 0.28	25.8 ± 0.56	28.1 ± 0	65.5 ± 0.06
ND3	31.0 ± 0.16	77.0 ± 0.34	38.3 ± 0.17	12.9 ± 0.14	14.7 ± 0.58	23.0 ± 0.01	46.2 ± 0.05
ND4	33.3 ± 0.14	73.5 ± 0.44	33.9 ± 0.12	15.2 ± 0.61	15.1 ± 0.52	35.5 ± 0.2	57.8 ± 0.07

Sa Staphylococcus aureus (ATCC 29213), *Mrsa* Methicillin-resistant *S. aureus* (ATCC 43300), *Ef Enterococcus faecalis* (ATCC 29212), *Ec Escherichia coli* (ATCC 25922), *Pa Pseudomonas aeruginosa* (ATCC 27853), *Kp Klebsiella pneumoniae* (ATCC 700603), *Ca Candida albicans* (ATCC10231)

Table 6 The molecular docking results

Compounds	DS[a]	E_{vdW}[a]	E_{Coul}[a]	E_{Total}[a]	RMSD
ND1	−5.609	−32.782	−1.051	−33.833	44.257
ND2	−5.660	−32.413	−2.457	−34.870	44.405
ND3	−5.442	−32.345	−1.088	−33.432	43.761
ND4	−6.150	−36.061	−1.142	−37.203	45.716

[a]In kcal/mol

that these compounds show activity as an antibiofilm agent [25]. In another study, it was reported that nicotinamide caused a reduction and destruction of the biofilm form of *Cutibacterium acnes* [26].

In summary, it was determined that the newly synthesized compounds have a remarkable antimicrobial activity against the tested microorganisms in this study. In addition, due to the moderate to strong biofilm inhibition results of these compounds, these substances are considered promising for the development of new antibiofilm agents.

Molecular docking

Antibacterial activity of studied compounds is investigated using molecular docking calculations against *E. Faecalis*. For this aim, 6QXS is selected as target protein. All calculations are performed at OPLS4 method with pH = 7 ± 2. The

Protein Structure

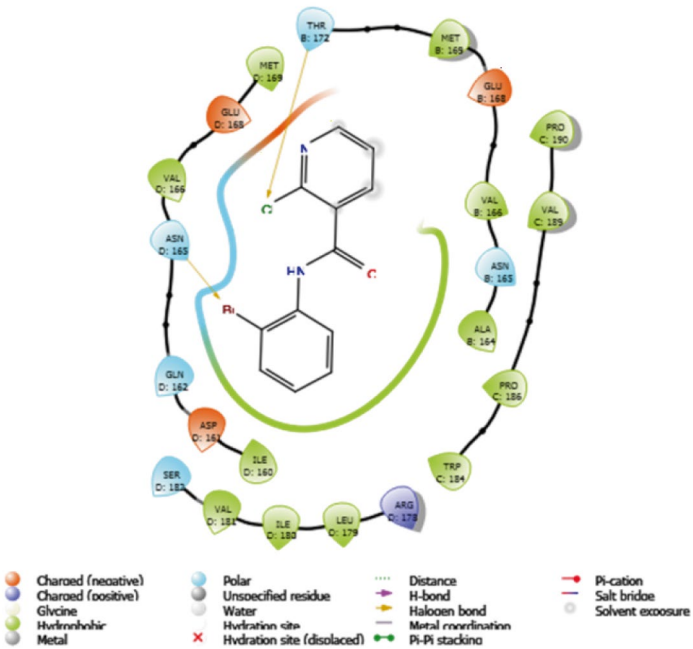

Interaction Map

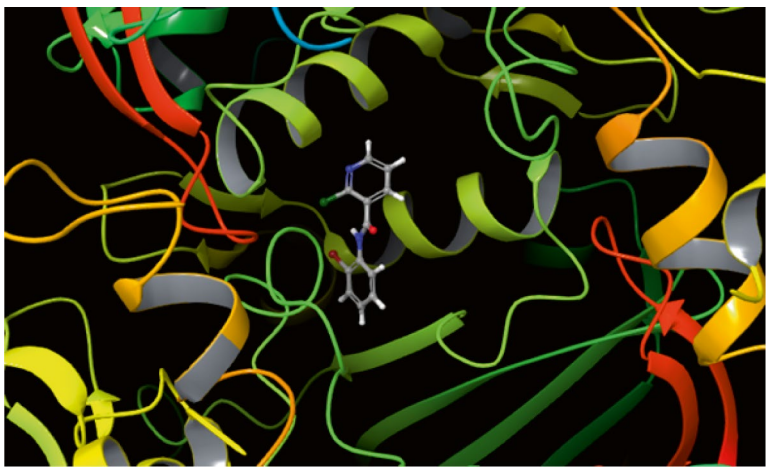

Complex Structure

Fig. 5 The protein structure of 6QXS, complex structure, and interaction map for ND4 compound

docking results, docking score (*DS*), van der Walls energy (E_{vdW}), Coulomb energy (E_{Coul}), and total interaction energy (E_{Total}) are summurized at Table 6.

According to Table 6, the best result is observed in ND4 compound due to the fact that the whole parameters except Coulomb energy are better than those of others. Additionally, key-lock harmony between inhibitor candidate and target protein is the best for ND4 compounds. Furthermore, the best interaction energy is obtained in ND4, too. Furthermore, RMSD values for the studied compounds are calculated and the highest value is obtained in ND4. It can be said that ND4 have better interaction with receptor binding domain of target protein. The structure of protein, complex (ligand–protein), and interaction map are represented in Fig. 5.

As a result, ND4 compound is found as the good inhibitor candidate. Additionally, obtained results via in silico analyses are good agreement with results of experimental studies.

Conclusion

Newly designed four nicotinamide derivatives which are 2-chloro-*N*-(2-chlorophenyl)nicotinamide, 2-chloro-*N*-(3-chlorophenyl)nicotinamide, 2-chloro-*N*-(4-chlorophenyl) nicotinamide, and N-(2-bromophenyl)-2-chloronicotinamide are synthesized and characterized by spectral techniques. Additionally, these compounds are optimized at B3LYP/6–31 + G(d,p) level in water and structural, electronic properties of them are examined in detail. Contour plot of frontier molecular orbitals and MEP maps of studied compounds are used in the determination of electronic properties. Antibacterial and antibiofilm properties of these compounds are investigated experimentally against numerous bacteria. The best antibacterial activity is observed in ND4. Finally, molecular docking calculations are performed against *E. Faecalis*. In this analysis, ND4 is found as the best one. Experimental results are supported by computational analyses.

Supplementary information The online version contains supplementary material available at https://doi.org/10.1007/s11224-022-01927-x.

Acknowledgements This research was made possible by TUBITAK ULAKBIM, High Performance, and Grid Computing Center (TR-Grid e-Infrastructure).

Author contribution AHTK performed the in vitro studies and manuscript preperation. GT performed experimental studies. EG performed the computational studies. RA performed the in vitro studies. KS FL designed the experiments and consistent guidance; analyzed the data, manuscript preparation, and review; edited the fnal version; and submitted it for publication. BT performed the in silico studies. HA designed the experiments and provided consistent guidance and manuscript preparation and review.

Funding This work is supported by the Scientific Research Project Fund of Sivas Cumhuriyet University under the project numbers RGD-020 and RGD-036.

Availability of data and material All experimental data were included in the article.

Declarations

Competing interests The authors declare no competing interests.

References

1. Knip M, Douek IF, Moore WPT, Gillmor HA, McLean AEM, Bingley PJ, Gale EAM (2000) Safety of high-dose nicotinamide: a review. Diabetologia 43:1337–1345
2. Köse DA, Necefoğlu H (2008) Synthesıs and Characterization of bis(nicotinamide) M-hydroxybenzoate complexes of Co(II), Ni(II), Cu(II) and Zn(II). J Therm Anal Calorim 93(2):509–514
3. Ye YH, Ma L, Dai ZC, Xiao Y, Zhang YY, Li DD, Wang JX, Zhu HL (2014) Synthesis and antifungal activity of nicotinamide derivatives as succinate dehydrogenase ınhibitors. J Agric Food Chem 62:4063–4071
4. Girgis AD, Hosni HM, Barsoum FF (2006) Novel synthesis of nicotinamide derivatives of cytotoxic properties. Bioorg Med Chem 14:4466–4476
5. Kolb H, Burkart V (1999) Nictinamide in Type I Diabetes. Diabetes Care 22:B16–B20
6. Eugen J, Marian K, Milan M, Jerzy M (1996) Structural Investigation of nickel(II)-nicotinamide-solvent interactions in solid complexes. Crystal structure of [Ni(H2O)4(NA)2](NO3)2·2H2O. J Coord Chem 40(3):167–176
7. Maiese K, Chong ZZ (2003) Nicotinamide: necessary nutrient emerges as a novel cytoprotectant for the brain. Trends in Pharmacological Science 24(5):228–232
8. Elliott RB, Pilcher CC, Fergusson DM, Stewart AW (1996) A population based strategy to prevent ınsulin-dependent diabetes using nicotinamide. J Pediatr Endocrinol Metab 9:501–509
9. Gale EAM, Bingley PJ (1994) Can We Prevent IDDM? Diabetes Care 17(4):339–344
10. Yang J, Klaidman K, Adams JD (2004) Update to medicanal chemistry of nicotinamide in the treatment of ıschemia and reperfusion. Med Chem Rev 1:13–17
11. Dennington R, Todd KA, Millam JM (2016) GaussView, Version 6.1, Semichem Inc., Shawnee Mission, KS
12. Frisch MJ, Trucks GW, Schlegel HB, Scuseria GE, Robb MA, Cheeseman JR, Scalmani G, Barone V, Petersson GA, Nakatsuji H, Li X, Caricato M, Marenich AV, Bloino J, Janesko BG, Gomperts R, Mennucci B, Hratchian HP, Ortiz JV, Izmaylov AF, Sonnenberg JL, Williams-Young D, Ding F, Lipparini F, Egidi F, Goings J, Peng B, Petrone A, Henderson T, Ranasinghe D, Zakrzewski JV, Gao J, Rega N, Zheng G, Liang W, Hada M, Ehara M, Toyota K, Fukuda R, Hasegawa J, Ishida M, Nakajima T, Honda Y, Kitao O, Nakai H, Vreven T, Throssell K, Montgomery JA, Peralta JE, Ogliaro F, Bearpark MJ, Heyd JJ, Brothers EN, Kudin KN, Staroverov VN, Keith TA, Kobayashi R, Normand J, Raghavachari K, Rendell AP, Burant JC, Iyengar SS, Tomasi J, Cossi M, Millam JM, Klene M, Adamo C, Cammi R, Ochterski JW, Martin RL, Morokuma K, Farkas O, Foresman JB, Fox DJ (2016) Gaussian 16, Revision B.01, Gaussian, Inc., Wallingford CT

13. Perkin E (2012) ChemBioDraw Ultra Version (13.0.0.3015)
14. Eloff JN (1998) A sensitive and quick microplate method to determine the minimal ınhibitory concentration of plant exctracts for bacteria. Planta Med 64:711–713
15. Celik C, Tutar U, Karaman İ, Hepokur C, Ataş M (2016) Evaluation of the antibiofilm and antimicrobial properties of Ziziphora tenuior L essential oil against multidrug resistant Acinetobacter baumannii. Int J Pharmacol 12(1):28–35
16. Onsare J, Arora D (2015) Antibiofilm potential of flavonoids extracted from Moringa oleifera seed coat against Staphylococcus aureus, Pseudomonas aeruginosa and Candida albicans. J App Microbiol 118(2):313–325
17. Friesner RA, Murphy RB, Repasky MP, Frye LL, Greenwood JR, Halgren TA, Sanschagrin PC, Mainz DT (2006) Extra precision glide: docking and scoring ıncorporating a model of hydrophobic enclosure for protein-ligand complexes. J Med Chem 49:6177–6196
18. Schrödinger Release 2021–2 (2021) Epik, Schrödinger, LLC, New York, NY
19. Schrödinger Release 2021–2 (2021) Protein Preparation Wizard; Epik, Schrödinger, LLC, New York, NY, 2021; Impact, Schrödinger, LLC, New York, NY; Prime, Schrödinger, LLC, New York, NY
20. Schrödinger Release 2021–2 (2021) SiteMap, Schrödinger, LLC, New York, NY
21. Pozzi C, Ferrari S, Luciani R, Tassone G, Costi MP, Mangani S (2019) Structural comparison of enterococcus faecalisand human thymidylate synthase complexes with the substrate dUMP and ıts analogue FdUMP provides hints about enzyme conformational variabilities. Molecules 24(7):1257
22. Vestbyv LK, Gronseth T, Simm R, Nesse LL (2020) Bacterial biofilm and its role in the pathogenesis of disease. Antibiotics (Basel, Switzerlard) 9(2):s59
23. Dang T, Nizamov IS, Salikhov RZ, Sabirzyanova LR, Vorobey VV, Burganova TI, Shaidoullina MM, Batyeva ES, Cherkasov RA, Abdullin TI (2019) Synthesis and characterization of pyridoxine, nicotine and nicotinamide salts of dithiophosphoric acids as antibacterial agents against resistant wound infection. Bioorg Med Chem 27(1):100–109
24. Adamiec M, Adamus J, Ciebiada I, Denys A, Gebicki J (2006) Search for drugs of the combined anti-inflammatory and antibacterial properties: 1-methyl-N' (hydroxymethyl)nicotinamide. Pharmacol Rep 58:246–249
25. Kumar RN, Mallareddy G, Nagender P, Rao PS, Poornachandra Y, Ranjithreddy P, Narsaiah B (2016) Synthesis of novel triazole functionalized pyridine derivatives as potential antimicrobial and anti-biofilm agents. Indian J Chem Sect B 55B:1361–1375
26. Shih YH, Liu D, Chen YC, Liao MH, Lee WR, Sheh SC (2021) Activation of deoxyribonuclease ı by nicotinamide as a new strategy to attenuate tetracycline-resistant biofilms of Cutibacterium acnes. Pharmaceutics 13:819